

Yuzhou Wu / Tanja Weil

# Nanodiamonds for Biological Applications

DOI: 10.1515/psr-2016-0104

## 8.1 Introduction

Nanodiamonds (NDs) represent a new class of carbon nanoparticles with unique physical and chemical properties. They are nanometer-sized carbon crystals with highly stable  $sp^3$  carbon in the core and reactive  $sp^2$  and amorphous carbons on the surface. The production of NDs is mainly from two methods, namely high-temperature/high-pressure (HTHP) synthesis and detonation method. The detonation method allows producing large quantities of NDs with low cost [1]. However, the detonation NDs normally provide single-digit nanometer sizes and form aggregation clusters in solution. The HTHP-synthesized NDs could be produced with different sizes ranging from a few nanometers to micrometers with highly crystalline structure [2]. A perfect diamond crystal is transparent to visible light. However, on rare occasions, natural diamond is found to display vivid color due to substitutional and vacancy defects in the lattice structure that are capable of absorbing and emitting visible light [3]. These defects could also be produced with synthetic NDs to obtain fluorescent NDs (FNDs) with desired optical properties. The most common and well-studied color center is the nitrogen-vacancy (NV) center [4] that offers spin-dependent photoluminescence. The NV center is a point defect in the diamond lattice that consists of a substitutional nitrogen atom that is directly adjacent to a lattice vacancy (Figure Figure 1). The fluorescence from the NV center is independent of the size of the host diamond particles (Figure Figure 1), and it is extremely stable without bleaching or blinking, which even allows their long-term observation at the single particle level in live cells [5]. Therefore, FNDs are particularly attractive for bioimaging applications. In addition, both the ground and excited states of the NV center display unique spin states with remarkably long coherence ( $T_2$ ) and relaxation times ( $T_1$ ), which are particularly attractive for developing sensitive magnetic and electron spin sensing in biological samples [6]. Recent studies suggest that NDs offer promising biocompatibility particularly in comparison with other fluorescent nanoparticles consisting of metals [7]. Taking together all these attractive features, NDs have emerged as promising nanoparticles for biological applications ranging from drug delivery to biosensing and theranostics [8]. The recent developments in this field will be discussed in this chapter.

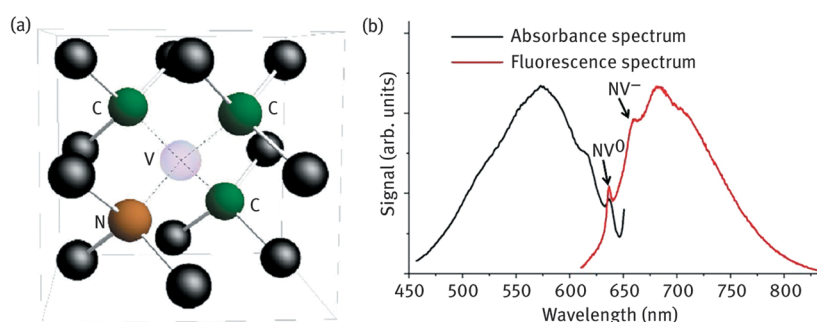


**Figure 1:** (a) The NV center in diamond – a substitutional nitrogen atom adjacent to a vacancy formed by a missing carbon atom. (b) The absorbance and fluorescence spectrum of an NV center.

## 8.2 Biocompatibility of NDs

Diamonds are generally considered stable, bioinert and biocompatible [7] due to their highly stable chemical structure, which makes them attractive for biological applications. Unlike other fluorescent nanoparticles containing heavy metal elements, for example, quantum dots and gold nanoparticles, NDs are composed of

Tanja Weil is the corresponding author.

© 2017 Walter de Gruyter GmbH, Berlin/Boston.

This content is free.

carbon, which is compatible in live systems. In comparison to other carbon-based nanomaterials, for example, fullerenes and carbon nanotubes, NDs are considered one of the most biocompatible forms since they consist of  $sp^3$  carbon, which is relatively unreactive. The biocompatibility of NDs has been tested both in vitro in cell lines and in vivo in animal models. Most of these experiments gave positive results [7, 9], while some reports also indicated potential risks [10]. Notably, their biocompatibility seemed to depend on the properties of the ND material, such as size, surface functionalities and concentrations. Therefore, the data from a particular experiment can only indicate the biocompatibility of a certain type of NDs. Optimization of the production and purification methods as well as surface functionalization could further improve the biocompatibility of ND materials.

### 8.2.1 In Vitro Biocompatibility Evaluation of NDs

Many in vitro cytotoxicity studies suggest that in comparison to other nanomaterials such as carbon nanotubes, semiconductor or metal particles, NDs represent the most biocompatible materials with no cytotoxicity to different cell lines [7, 9]c, d]. Schrand et al. [9]d] compared the biocompatibility of different carbon nanomaterials in aqueous suspensions, such as detonation NDs, single- and multi-walled carbon nanotubes (SWNTs and MWNTs) and carbon black (CB), in both neuronal and lung cell lines at concentrations ranging from 25 to 100  $\mu\text{g/mL}$  for 24 h. The biocompatibility was evaluated with regard to the morphological and subcellular effects of these nanomaterials on mitochondrial membrane permeability and reactive oxygen species generation [9]d]. The greatest biocompatibility was found after incubation with NDs and both cell types followed the trend: ND > CB > MWNT > SWNT [9]d]. In another study [7], they have also shown that NDs with different surface functionalities, such as  $-\text{COOH}$ ,  $-\text{COO}^-\text{Na}^+$ ,  $-\text{SO}_3^-\text{Na}^+$ , are equally nontoxic in different cell lines, including even neuroblastoma and macrophages, which are normally much more sensitive to chemical reagents. Notably, in these experiments detonation NDs with sizes ranging from 2 to 10 nm were applied that are known to form aggregates in blood circulation and they do not exist as individual particles [11]. In another study, Liu et al. [9]c] tested carboxylated NDs (cNDs) with 5 and 100 nm sizes and also compared their toxicity with carbon nanotubes [12]. They found that nanotubes induced cytotoxicity in human lung cells. However, treatment with NDs of both sizes did not induce cell death and apoptosis, although cND particles were retained in lung cells. Furthermore, cNDs did not alter the protein expression profile in these cells [12]. The 100 nm cNDs were taken into cells by macropinocytosis and clathrin-mediated endocytosis pathways. Even after long-term cell culture for 10 days in both A549 lung cancer cells and 3T3-L1 embryonic fibroblasts, no toxicity was observed. Cell division into two daughter cells was unaffected by the presence of cNDs. Finally, the cells retained NDs in the cytoplasm after cultivation for several generations without interfering with gene or protein expression on the regulation of cell cycle progression and adipogenic differentiation [12]. However, genotoxicity studies of detonation NDs with embryonic stem cells indicated that NDs induce slightly increased expression of DNA repair proteins (p53 and MOGG-1) and the oxidized NDs might cause more DNA damage than the pristine NDs. Though compared to other carbon nanomaterials such as nanotubes, the DNA damage caused by NDs is considered less severe [10]a].

### 8.2.2 In Vivo Biocompatibility Evaluation of NDs

A few studies have also investigated NDs in living animal models, such as in rats and *Caenorhabditis elegans* (*C. elegans*) [9]a, b]. The long-term stability and biocompatibility of 100 nm FNDs in rats through intraperitoneal injection was investigated over 5 months. Histopathological analysis of various tissues and organs indicated that FNDs are nontoxic even at very high dosing of up to 75 mg/kg body weight. The measurements of water and fodder consumption, body weight, and organ index also revealed no significant differences between the control and FND-treated groups [9]a]. Another study reported long-term in vivo imaging of FNDs (0–10 nm) in *C. elegans* by either feeding them with a colloidal FND solution or microinjecting an FND suspension into the gonads of the worms [9]b]. On feeding, bare FNDs remained in the intestinal lumen, while FNDs conjugated with biomolecules (such as dextran and bovine serum albumin) were absorbed into the intestinal cells. On microinjection, FNDs were dispersed in the gonads and delivered to the embryos and eventually into the hatched larvae of the next generation. The toxicity assessments, performed by employing longevity and reproductive potential as physiological indicators and measuring stress responses with use of reporter genes, suggested that FNDs are stable and nontoxic and do not cause any detectable stress to the worms [9]b]. Therefore, the combination of many attractive features such as biocompatibility and high chemical and photophysical stability points to a promising applicability of NDs as contrast agents for long-term in vivo imaging.

Similar as other nanomaterials, one potential risk of NDs could be the long-time accumulation in liver, spleen and lung due to slow excretion rates [10]b]. However, based on the thus far observed low toxicity, ad-

ministration of NDs in vivo with small dosage is still promising. In addition, NDs of different sizes, surface modifications and administration routes will most likely also have an impact on their biodistribution. Therefore, by tuning the size distribution, enhancing the colloidal stability and optimizing the surface functionalities, the in vivo performance of NDs could be improved and adjusted to the respective in vivo requirements.

### 8.3 Surface Coating for Improving ND Stability and Biocompatibility in Biological Environments

The raw, as-synthesized NDs easily form aggregates especially in biological media due to their large surface to volume ratio, which could be one reason for long-term toxicity [11]. Although direct treatment of NDs surface, for example, oxidation, could improve the colloidal stability in aqueous solution [13], coating NDs with a biocompatible shell, such as a polymer shell, is still the most efficient strategy to avoid aggregation in complicated biological environments. With different properties of the coating materials, the biocompatibility and biodistribution of NDs could also be flexibly optimized. The coating of NDs could be achieved by covalent conjugation or non-covalent interaction. In addition, a silica shell could also be grown outside NDs to change their surface properties. A direct comparison of these approaches is given below.

#### 8.3.1 Covalent Coating of NDs

The  $sp^2$  carbon on the ND surface could be oxidized to impart functional groups such as hydroxyl groups and carboxylic acid groups. Thus, polymers could be directly attached to these functionalities to form a protecting outer shell. Polyethylene glycol (PEG) is one of the most widely used polymers for this purpose, including linear PEG, branched PEG and polyglycerol, which is known to provide a highly hydrated shell with low immunogenicity and low plasma protein adsorption [14]. The conjugation of PEG and its derivatives to NDs could be achieved by both “grafting to” and “grafting from” strategies [15] (Figure Figure 2(a)). The “grafting to” method allows fast conjugation of different types of PEG-like polymers directly on the surface functional groups of NDs (e.g., carboxylic acid groups) and the polymer length could be rationally selected and well characterized before conjugating to NDs. The limitation of this method is a relatively low polymer density, which might result in insufficient protection of the inner ND core. For instance, PEG4000 was conjugated to NDs by the “grafting to” strategy, which could reduce the high tendency for aggregation of pristine ND and small clusters were obtained in phosphate buffered saline (PBS) and cell culture medium [15]b]. However, the coated NDs still precipitated from aqueous solution after some time [15]a] (Figure Figure 2(b)). To achieve even more stable polymer coatings, the “grafting from” strategy turned out beneficial to obtain a denser shell. By atom transfer radical polymerization, a poly(PEG methyl ether methacrylate) layer could be grown on NDs. The resulting NDs were much more stable in organic and aqueous solution with negligible precipitation after 22 h [15]a] (Figure Figure 2(b)). Polyglycerol could also be grafted on NDs via ring opening polymerization [16]. The coated NDs are highly stable in aqueous condition, which allows size exclusion purification to achieve really narrowly distributed NDs. The purified NDs appeared as single particles on transmission electron microscope (TEM) without aggregations. Due to the high number of hydroxyl groups on the polyglycerol layer, these NDs could be easily functionalized with desired functional entities, such as anticancer drugs [15]c]. Drug delivery applications will be discussed in later sections. Another special type of “grafting from” strategy is based on the biomimetic dopamine self-polymerization. Dopamine [17] (Figure Figure 2(c)), chemically known as 4-(2-aminoethyl)benzene-1,2-diol, is one of the crucial catechol amine neurotransmitters that is widely distributed in mammalian brain tissues. In addition, it is also a biomimetic anchor for the functionalization of surfaces due to its self-polymerization nature under oxidative condition. The hydroxyl group on ND surface could be covalently reacted with dopamine during their self-polymerization process, thus resulting in a stable covalent coating of dopamine polymer on ND. By using dopamine derivatives with functional groups, this method could be a simple and a versatile strategy to functionalize ND surfaces with hydroxyl groups, azide groups and even poly-*N*-isopropylacrylamide [17].

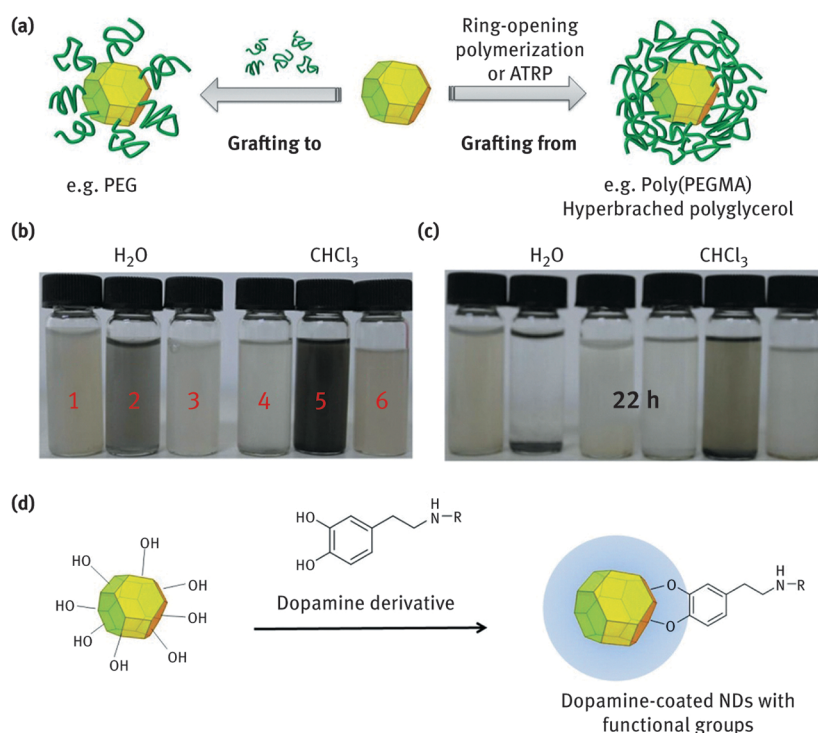


**Figure 2:** Methods for covalent coating of NDs with polymers. (a) Illustration of “grafting to” and “grafting from” methods for the preparation of PEG-like polymer coatings. (b) and (c) Photographs of raw NDs (1,4), PEG-coated NDs prepared by the “grafting to” strategy (2,5), and poly(PEGMA)-coated NDs prepared by the “grafting from” strategy (3,6) in water and chloroform at room temperature upon mixing and after 22 h. (d) Preparation of dopamine-coated NDs. (b) and (c) are reprinted from Ref. [15]a) with permission.

### 8.3.2 Non-covalent Coating of NDs

NDs could also be coated by non-covalent interactions, which is the primary method to bring a protein coating onto NDs. It has been demonstrated that NDs, after oxidization in strong acid, could have very high affinity to various types of proteins, such as cytochrome c, myoglobin and albumin [18]. This is an integrated result from electrostatic forces, hydrogen bonding and hydrophobic interactions. In this way, NDs could absorb a layer of bovine serum albumin (BSA) or α-lactalbumin [18]. The stimulated emission depletion (STED) microscopy has shown that the albumin-coated NDs could be taken up into cells and homogeneously distributed without aggregation inside live cells [19]. However, the major limitation of non-covalent absorption is the stability of the coated layer, especially in complicated environments. Introducing multivalent interactions might be a possibility to overcome this limitation. For instance, the highly positively charged polyelectrolyte polyethyleneimine (PEI) could interact strongly with negatively charged NDs to form a stable complex for gene delivery [20]. However, the random electrostatic interaction between PEI and NDs creates inhomogeneous clusters instead of coating of single particles. Recently, an innovative concept based on a multivalent polymer [21a] as well as polypeptide biopolymer coating derived from the human blood plasma protein albumin was proposed [21b] (Figure Figure 3(a)). The biopolymer was obtained after unfolding native serum albumin in urea and in situ attachment of PEG to the thiol groups reduced from disulfide bridges [22] (Figure Figure 3(a)). All the carboxylic acid groups from native albumin were converted to primary amine groups in this biopolymer, thus allowing efficient multivalent electrostatic interactions with the negatively charged ND surface. The PEG side chains decrease aggregations of the particles. Therefore, NDs coated by this biopolymer were found to be extraordinarily stable inside different kinds of aqueous buffers, including PBS, cell culture medium and even 1 M NaCl solution [21b] (Figure Figure 3(c)). This biopolymer offers high numbers of orthogonal functional groups, which allow attachment of different active components onto coated NDs. This has been demonstrated by attaching drug molecules for anti-tumor drug delivery [21b]. Particularly, even after loading of high numbers of hydrophobic drug molecules (doxorubicin, DOX), NDs were still found to be extremely stable in all physiological media. Moreover, due to the biocompatibility of the biopolymer and the high colloidal stability, the coated NDs showed no cytotoxicity even with concentrations as high as 3 mg/mL [21b].

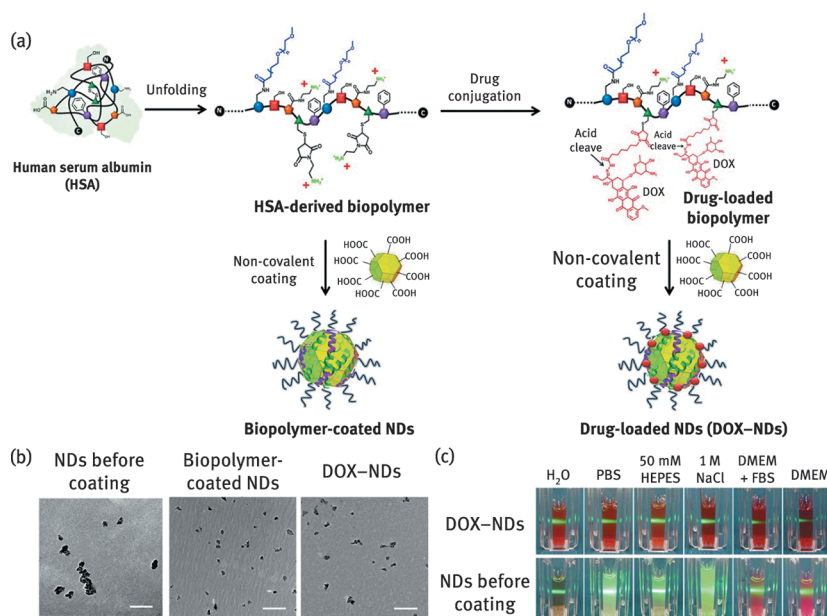


**Figure 3:** (a) Preparation of NDs coated with albumin-derived biopolymer and loading of anticancer drug doxorubicin (DOX). (b) Transmission electron microscope image of NDs before coating, after biopolymer coating and after DOX loading. Scale bar: 200 nm. (c) Photographs of 1 mg/mL DOX-NDs and raw NDs suspended in different physiologically relevant solutions, respectively. The green laser beam does not scatter in DOX-ND samples and in ND aqueous solution indicating no visible particle aggregation in solution. In contrast, the laser beam strongly scatters in raw ND samples suspended in PBS, 50 mM HEPES pH 7.5, 1 M NaCl and DMEM (Dulbecco's modified Eagle's medium) with/without 20 % fetal bovine serum (FBS) due to aggregate formation. Reprinted from Ref. [21]b] with permission.

### 8.3.3 Silica Coating

Another strategy to functionalize ND surface focuses on growing an inorganic shell. For instance, NDs could be encapsulated with a silica shell by either direct silica shell growth from an ND core or by liposome-based encapsulation processes [23] (Figure Figure 4). Cigler et al. demonstrated a multiple layer coating method to cover NDs with a first silica shell layer, a second layer of thin cross-linked aminopropyl-silica shell and a third layer of PEG with ethynyl end groups (Figure Figure 4(b)). By this method, the obtained NDs are stable over a broad pH range (pH 2–10) and even in 1 M NaCl and cell culture medium [24]. This method also provides a high density of ethynyl functional groups on the surface that could allow efficient click reaction to achieve more than 2,000 dyes or peptides on an individual ND. Similarly, if the first layer of the silica shell contains methacrylate, the second layer could also be a polymeric layer by direct in situ radical polymerization [25]. In addition, a liposome-based method was reported by Neuman et al. [23] to decorate NDs with a silica shell (Figure Figure 4(a)). The liposomes help to select for a desired size of particles, thus producing nearly monodispersed particles after coating that is independent of the surface properties of original NDs [23]. The silica shell imparts an anionic character and stable, monodispersed NDs were achieved over a relevant working pH range (pH = 5–8), particularly in the pH range above 3, where the strong negative zeta potential (−35 mV) allowed the particles to have strong electron repulsion, thus obtaining high colloidal stability [23].

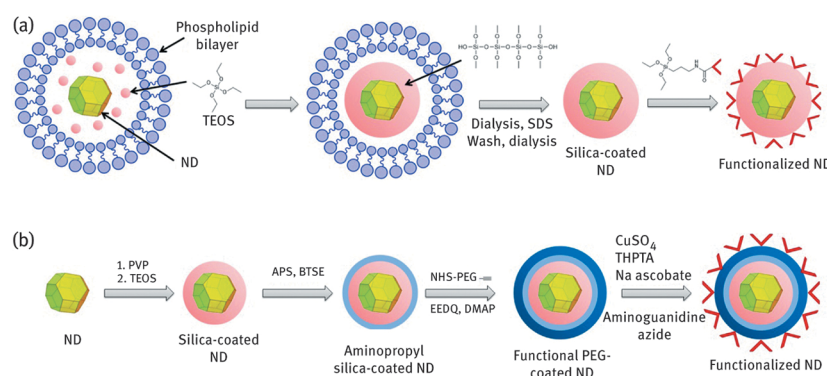


**Figure 4:** Preparation of silica-coated NDs via (a) liposome-based method and (b) multilayer coating. TEOS, tetraethoxysilane; BTSE, 1,2-bis(triethoxysilyl)ethane; APS, (3-aminopropyl)triethoxysilane; PVP, polyvinylpyrrolidone; EEDQ, 2-ethoxy-1-ethoxycarbonyl-1,2-dihydroquinoline; DMAP, dimethylaminopyridine.

## 8.4 Functionalization of NDs with Biomolecules

To advance the biological applications of NDs, another essential step is to attach biomolecules of interest onto NDs. Several methods to attach biomolecules, such as proteins and DNAs, to NDs for protein delivery, gene delivery and biosensing have been already reported, which will be discussed in this section.

### 8.4.1 Introduction of Proteins onto NDs

The most straightforward method to attach proteins onto NDs is physical adsorption. The large surface to volume ratio allows efficient adsorption of proteins. In addition, the functional groups at the ND surfaces, such as hydroxyl groups and carboxyl groups, could also provide electrostatic interactions and hydrogen binding with proteins. By integration of all these effects, the physical adsorption of proteins on NDs could be sufficiently stable for many desirable applications such as protein delivery, cell targeting and sensing. For instance, the therapeutic protein insulin was adsorbed to detonation NDs, thus forming insulin–ND complexes [26]. The adsorbed insulin could also be released under alkaline conditions [26]. Cell viability assays and real-time polymerase chain reaction quantifying the expression of *Ins1* and *Csf3/G-csf* gene revealed that ND-bound insulin remained inactive while the desorbed insulin could recover their activity [26]. These results suggest great potential of NDs as facile platform for protein delivery. The HTHP NDs with average sizes of around 100 nm could also adsorb proteins through the interplay of electrostatic forces, hydrogen bonding and hydrophobic interactions [27]. By adsorbing different proteins, the modified NDs could be taken up selectively by a specific cell type for targeted cell imaging [27]. The physical adsorption approach has also facilitated sensing of proteins. For instance, ferritin was adsorbed on NDs with stable NV centers. Using the magnetosensing techniques with NV centers (see Section 8.5.2), the iron concentration inside the ferritin could be detected without damaging the protein cage [28].

However, to achieve more stable and specific binding of proteins to NDs, covalent conjugation is still a more reliable strategy in comparison to physical adsorption. By direct functionalization of NDs with different functional groups, proteins could be covalently conjugated to ND surfaces [8]c, [29]. For instance, thiolated antibodies could be conjugated to thiol-reactive *N*-succinimidyl 3-(2-pyridyldithio) propionate (SPDP)-modified NDs [30]. However, it should be noted that direct chemical modification of NDs often leads to agglomeration. If well-dispersed individual ND particles are desired, it is necessary to conjugate the proteins on polymer-coated NDs. For instance, NDs could be first coupled with functionalized PEG, which could on the one hand impart improved stability of the NDs and, on the other hand, allow easy conjugation of proteins. Streptavidin was conjugated to the functionalized PEG to further serve as an adaptor. Thus, commercially available biotinylated antibodies could be quickly labeled onto these NDs for immunostaining [27]. Notably, even if PEG linker is used, small amounts of agglomeration are still difficult to avoid. It was necessary to perform the labeling experiment with inversed cell culture to avoid deposition of such aggregates on the cell surface [27]. The coating strategies discussed above could provide novel opportunities to achieve more stable protein functionalized NDs, which still need to be further tested.

### 8.4.2 Modification of DNA on NDs

In comparison to the preparation of protein-modified NDs, it is even more challenge to prepare DNA-functionalized NDs with high colloidal stabilities. For some applications, such as gene delivery or drug delivery, controlled small agglomeration is not problematic. In these cases, the modification of NDs with DNA molecules could also be achieved by simply physical adsorption or direct covalent conjugation. For instance, highly positively charged polymer PEI was coated onto acid-treated NDs via electrostatic interaction to cover the NDs with high density of positive charges. Thus, negatively charged DNA plasmids formed dense complexes with PEI-coated NDs, which have shown high gene transfection efficiency with relatively low cytotoxicity [20]. Thiolated synthetic ssDNA was also covalently conjugated to SPDP-modified NDs similarly for protein conjugation [30]. However, both methods do not allow producing NDs with sufficient colloidal stability for advanced biosensing applications, where individual ND particles are preferred.

Recently, following the biopolymer coating strategy introduced above, highly stable NDs functionalized with DNA were achieved [31] (Figure Figure 5). Biotinylated PEG was used as biopolymer side chains, which formed a biotin-functionalized shell on coated NDs. Thus, the streptavidin adaptor could be assembled on the NDs, which allowed easy conjugation of biotinylated ssDNA. Since the biopolymer coating is highly stable with excellent water solubility, single ND particles were found even after all these functionalization steps [31]. This achievement is particularly important for producing high-quality biofunctionalized NDs for NV center-based high-resolution sensing techniques.

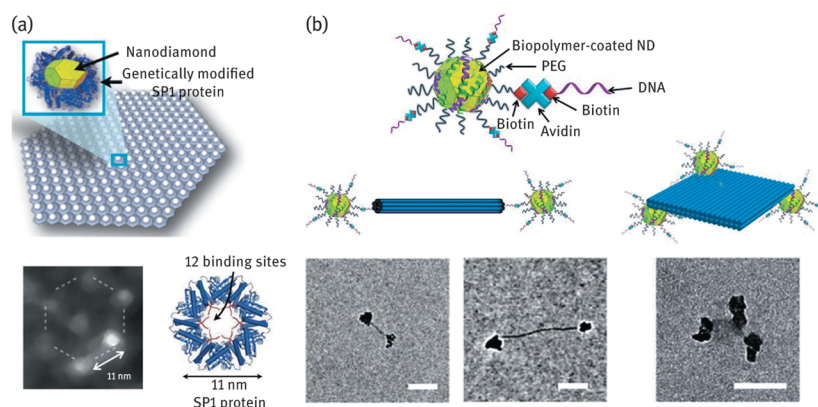


**Figure 5:** (a) ND arrays formed on genetic engineering SP1 proteins. The scheme above shows an ordered hexagonal array of SP1–ND hybrids consisting of an ND attached to the SP1 inner cavity. Here, the SP1-monolayer serves as a structural scaffold. The DF-STEM (dark-field scanning transmission electron microscopy) image shows a hexagonal structure formed of seven NDs (ND diameter  $\sim 5$  nm). The SP1–protein ring consists of binding sites that are genetically modified to enable graphite-specific binding. (b) NDs assembled on DNA origami with 2D and 3D structures. The NDs are coated with biopolymer and the PEG side chains are functionalized with biotin to form biotin–avidin–biotin linkers for DNA conjugation. The DNA-modified NDs are stable without aggregation and therefore could be assembled on DNA origami nanostructures with defined geometries. A 2D assembly was demonstrated with two NDs fixed on two ends of a DNA origami tube with defined length. A 3D assembly was demonstrated with three NDs attached on a DNA origami square. The TEM images show the self-assembled structures. Scale bar = 100 nm. The figure is partially reprinted from Refs [31, 32] with permission.

### 8.4.3 Self-Assembled NDs on Bionanostructures

One unique application of protein- and DNA-conjugated NDs is to prepare defined self-assembled ND arrays on bionanostructures. Periodic arrangements of NDs with NV centers are an essential and highly challenging step toward efficient quantum information processing, quantum simulation and quantum sensing applications [32]. To achieve this goal, a novel approach was developed recently based on the self-assembling capabilities of biological systems. Techniques from bionanotechnology exploit the self-assembling behavior of special designed protein and DNA to produce periodical structures with nanometer spatial resolution. Through the conjugation techniques available for connecting NDs with protein and DNA building blocks, one could incorporate NDs onto these bionanostructures to achieve a defined nanoarray. One example is the formation of small ND arrays on SP1 protein variant (Stable Protein 1, Figure Figure 5(a)), which could form numerous dimers and trimers along with large ordered structures such as a seven ND hexagon [32]. The emerging technique of DNA origami based on programmed folding of single-stranded DNA molecules allows creating even more complex structures ranging from periodic arrays to three-dimensional (3D) architectures [33] (Figure Figure 5(b)). This offers an ideal platform to assemble ND arrays with flexible distance and sophisticated nanostructures. To assemble NDs onto DNA origami particularly requires DNA functionalized NDs with high colloidal stability even under high ionic strength. The biopolymer coating strategy discussed above provides an ideal method to achieve DNA functionalized NDs sufficient for preparing NDs on DNA origami. It has been demonstrated that with this method, NDs could be self-assembled on DNA origami in predefined one-dimensional, two-dimensional (2D) and 3D geometries and defined distance [31] (Figure Figure 5(b)). These assemblies provide unique tools for studying self-assembled NV center spin lattices or plasmon-enhanced spin sensors as well as improving fluorescence labeling for bioimaging.

## 8.5 ND for Drug delivery

One major biological application of NDs is serving as drug delivery nanocarrier. ND-based drug delivery systems receive an increasing recognition due to their unique combination of promising biocompatibility and attractive optical properties. The highly stable emission of FNDs without bleaching and blinking enables long-time monitoring of the drug delivery process and drug release from the carrier. Therefore, using FNDs as nanomedicine platform for drug delivery into cancer cells and tissue would allow combining fluorescence-based tumor diagnostic and cancer therapy within one particle, which is essential for the evolving new concepts of “theranostic” (a portmanteau of therapeutics and diagnostics). The different strategies to achieve drug delivery with NDs will be discussed in this section.

### 8.5.1 Drug Delivery with Detonation ND Clusters

The first generation of ND–drug delivery systems has been prepared by simply absorbing mainly lipophilic drug molecules onto the ND surface [34]. These ND–drug complexes comprised of about 4–6 nm primary detonation ND particles clustered in solution into 100–200 nm aggregates, which can substantially absorb drug molecules and significantly enhance their blood circulation half-life and tumor retention [34, 35]. Dean Ho’s group has done intensive studies with this strategy. They investigated the absorption of hydrophobic anticancer drugs such as DOX [34, 35], purvalanol A, 4-hydroxytamoxifen [36] and mitoxantrone (MTX) [37], anti-inflammatory drug dexamethasone [37] and the diabetes drug insulin [26] onto the ND complexes. Delivering anticancer drugs with ND complexes was found to be able to circumvent drug resistance. A major mechanism for drug resistance is that the cells pump drugs out through ATP-binding cassette (ABC) transporters. They have shown that ND–drug complex could overcome the drug efflux via an ABC transporter-independent pathway [35a]. Both ND–DOX complex [35a] and ND–MTX complex [37] have shown significant improved drug retention in respective drug-resistant tumor cell line. They have also demonstrated in vivo that ND–DOX complex could significantly increase apoptosis and inhibit tumor growth in both murine LT2-Myc liver tumor and 4T1 mammary tumor without affecting adjacent normal tissues [35a] (Figure Figure 6). The reason for the advantages of ND–DOX complex over free DOX is proposed to be the gradual release of the drug from NDs, which allows for slow drug release over a long time to maintain the free DOX concentration below a toxic level to normal tissues.

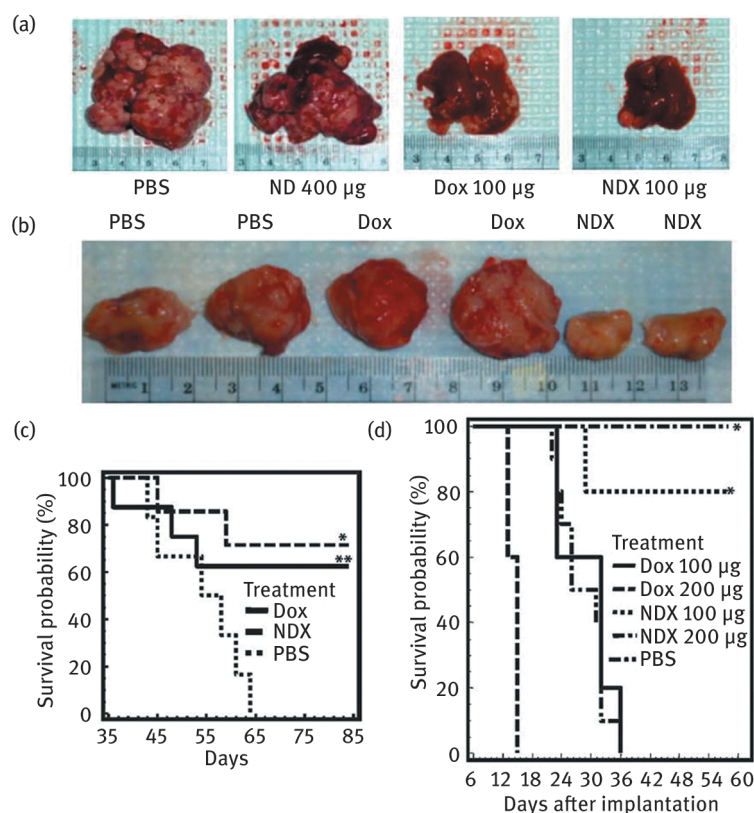


**Figure 6:** The in vivo test of DOX delivered by detonation NDs in (a) and (c) murine LT2-Myc liver model and (b) and (d) murine 4T1 mammary carcinoma model. (a) Representative images of livers/tumors from LT2-Myc mice. (b) Representative images of excised tumors from 4T1 mice. (c) Kaplan–Meier survival plot for LT2-Myc mice treated with PBS ( $n = 5$ ), Dox (100 mg) ( $n = 8$ ), or NDX (100 mg of Dox equivalent) ( $n = 7$ ) by tail vein injection every 7 days.  $*P < 0.03$ ;  $**P < 0.06$ . (d) Kaplan–Meier survival plot for 4T1 mice treated with PBS ( $n = 7$ ), Dox (100 mg) ( $n = 10$ ), NDX (100 mg of Dox equivalent) ( $n = 10$ ), Dox (200 mg) ( $n = 5$ ), or NDX (200 mg of Dox equivalent) ( $n = 5$ ) by tail vein injection every 6 days.  $*P < 0.003$  [35]a]. Reprinted from Ref. [35]a] with permission.

The simple absorption strategy is high throughput and universal to different types of therapeutics independent of their structure. However, the complexes are not really stable inside blood plasma and the nonspecific drug release is always difficult to avoid. Therefore, covalent linking of drug molecules to the detonation ND clusters was also investigated. By 1-Ethyl-3-(3-dimethylaminopropyl)-carbodiimide/*N*-Hydroxysuccinimide (EDC/NHS) coupling, DOX and cell penetration peptide TAT could be directly conjugated to the carboxylic acid groups on ND surface to enhance penetration of cell membrane [38]. PTX [39] has also been conjugated to the hydroxyl groups on NDs to avoid dissociation process. The activity of covalently linked PTX was maintained as shown by inducing mitotic arrest, apoptosis and anti-tumorigenesis of human lung cancer cells in xenograft severe combined immunodeficiency (SCID) mice. However, the mechanism of PTX release is unclear in this case. Dean Ho et al. [30] have reported a more sophisticated strategy to attach fluorescently labeled paclitaxel (PTX)–DNA conjugates and anti-EGFR antibody onto the ND surface. The PTX–DNA conjugates were covalently attached to ND surface via a disulfide linker, which allowed controlled drug release only under reducing condition. They have shown that these complexes could be efficiently taken up into epidermal growth factor receptor (EGFR) overexpressing cell lines and exhibited efficient therapeutic efficacy which was twofold increased comparing to nontargeted ND delivery system.

### 8.5.2 Drug Delivery with Polymer-Modified NDs

Although covalent linking of drug molecules could reduce drug leakage, the complex formation by random aggregation of the extremely small detonation ND particles is still an uncontrolled process, thus the clusters may not be stable during circulation. In addition, the NV centers in these small NDs are not stable; therefore, their optical property is not sufficient for high-quality bioimaging. Milling HPHT diamond could obtain more stable ND particles with sizes ranging from tens to hundreds of nanometers. Using single NDs as drug delivery carrier instead of their uncontrolled clusters is a strategy to achieve a well-defined drug delivery system. In addition, they could have multiple very stable NV centers, which are particularly attractive to develop as theranostic agents that combine drug therapy and diagnostic imaging in one particle. However, the bare NDs tend to form aggregations in the biological environment; therefore, single ND-based drug delivery normally requires a polymer coating on the ND surface as discussed in Section 8.3. For instance, polyglycerol-coated NDs with average size of 50 nm could be conjugated with Pt-based anticancer drug via pH-responsive linker [15]c]. As discussed earlier, ND coated with polyglycerol exhibits good solubility in a physiological environment and also provides a large number of hydroxyl groups that could be conjugated with drugs as well as Arg-Gly-Asp (RGD) peptide for tumor cell targeting. In vitro experiments showed that the Pt-RGD-conjugated NDs could be taken up by U87MG cells and induced high toxicity, but no uptake and toxicity effect was observed with HeLa cells, revealing the high targeting efficacy. The stable NV centers in these NDs allow fluorescence imaging of the drug delivery process in cells by confocal microscopy. Notably, the Pt complex is a water-soluble anticancer drug that will not reduce the solubility of drug-loaded NDs. To achieve high colloidal stability of NDs even after loading hydrophobic drugs still remains a key challenge since lipophilic groups at the ND surface usually promote the formation of larger aggregates [36]. Uncontrolled aggregation of nanoparticles has been connected with unexpected cell toxicities and the prevention of clogging capillary blood vessels is a critical concern for clinical development of nanomaterials [40].

Recently, the Cigler [21a] and the Weil group [21]b] prepared NDs with polymer [21a] and biopolymer [21]b] coatings biopolymer, which displayed excellent colloidal stability as discussed in Section 8.3 (Figure Figure 3). A defined number of DOX molecules could be conjugated onto the functional groups on the biopolymer before coating with NDs, thus the DOX-loading process could be precisely controlled and well characterized. Particularly, NDs coated with the DOX-loaded biopolymer are still highly stable without any aggregation under all physiological conditions tested (Figure Figure 3(c)). The biopolymer-coated NDs showed efficient cell uptake and excellent biocompatibility. Since high numbers of DOX molecules were linked to NDs by an acid-cleavable linker, they could be efficiently transported and released inside cancer cells [21]b] (Figure Figure 7(e)). They have also demonstrated the theranostic potential of this system by using FNDs with NV centers. The intracellular distribution of NDs and DOX was resolved in live cells by recording the fluorescence spectra of NDs and DOX in different cellular compartments [21]b] (Figure Figure 7(a–c)). Significant amounts of DOX were released

from ND carriers and distributed inside the cytoplasm and the nucleus, whereas the ND carriers remained entrapped inside endosomal [21]b (Figure Figure 7(a–c)). The antitumor efficacy was shown with in vitro cellular experiment as well as with chicken embryo models. The DOX-loaded NDs were found to have similar  $IC_{50}$  in comparison to free DOX in cellular experiments, but shown more efficient tumor inhibition in chicken embryo models due to tumor accumulation after longer blood circulation time [21]b (Figure Figure 7(d)). This strategy could be particularly attractive for developing multimodal NDs combining therapy and imaging potential in one particle for the emerging concept of “theranostics.”

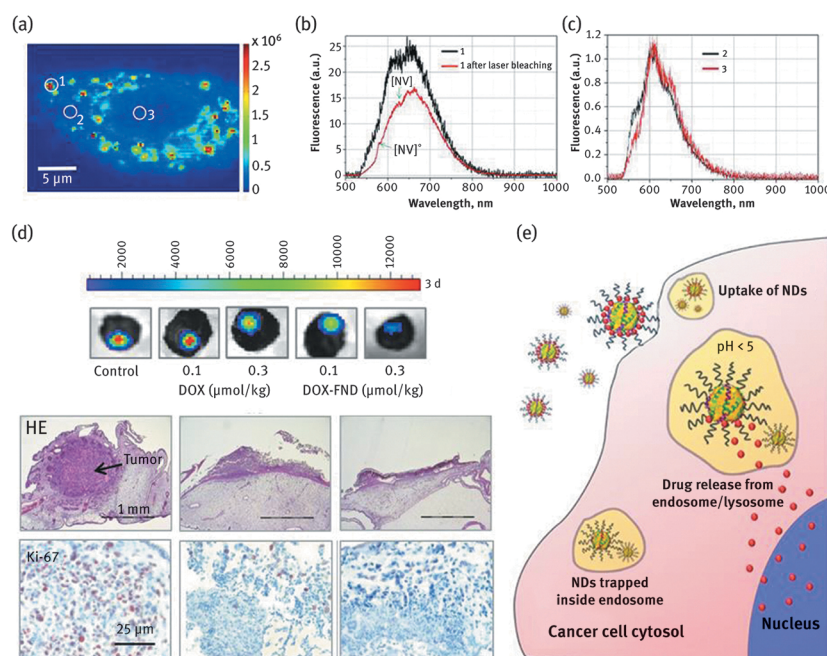


**Figure 7:** DOX delivery by biopolymer-coated NDs. (a) Fluorescence spectra inside living cells. A549 cells were treated with 55  $\mu\text{g}/\text{mL}$  of fluorescent DOX-NDs for 24 h. Fluorescence spectra were recorded at positions highlighted by white circles. (b) Representative emission spectra inside cellular vesicles (line 1), e.g., circle 1, corresponds to the overlapping spectra of DOX and N-V centers. The emission spectrum after laser bleaching (line 1 after laser bleaching) yielding a typical emission spectrum of N-V centers with assignable peaks from  $[\text{N-V}]^0$  and  $[\text{N-V}]^-$ . (c) The representative emission spectra within the cytosol (line 2), e.g., circle 2, and inside the nucleus (line 3), e.g., circle 3, both revealing typical DOX spectra. (d) Antitumor effect of DOX-NDs on breast cancer xenografts in chorioallantoic membrane (CAM) model. Photograph on top showing the representative tumor luminescence in CAM model. Photograph below showing the immunohistochemical analysis of breast cancer xenografts. HE, hematoxylin and eosin staining of whole xenografts grown on CAM; Ki-67 antigen staining of tumor xenografts, brown-red nuclei are indicative of proliferating cells. (e) Illustration of cell uptake and drug-release process of DOX-ND. Reprinted from Ref. [21]b with permission.

## 8.6 NDs for Imaging and Biosensing

The biocompatibility evaluation of NDs and their drug delivery studies supports the promising potential of using NDs in living biological systems. In addition, the unique fluorescence properties and electromagnetic properties of NV centers make NDs particularly attractive for biosensing. The fluorescence from NV centers is in the near-infrared region with extremely high photostability and sufficiently long lifetime, which makes them one of the best fluorescence labels for high-resolution fluorescence imaging. In addition, the ground and the excited states of the NV center display zero-field magnetic resonances at 2.88 and 1.42 GHz, respectively. Such magnetic resonance occurs between the  $m_s = 0$  and the  $m_s = \pm 1$  magnetic states of an electronic spin triplet (Figure Figure 8). This electron spin exhibits remarkably long coherence ( $T_2$ ) and relaxation times ( $T_1$ ), which can reach milliseconds in ultrapure diamond [6]. With a concept of single-molecule optically detected magnetic resonance [41], the electronic spin state of even a single NV center can be detected by means of electron spin state-dependent light scattering that discriminates between the  $m_s = 0$  and the  $m_s = \pm 1$  states [42]. These unique properties of NDs offer great potential to develop the smallest magnetosensing probes for detecting the tiniest of magnetic fields in vitro and in vivo. Moreover, the electron spin triplet to the  $m_s = 0$  state could be hyperpolarized by optical pumping even at room temperature, and this hyperpolarization could be transferred to nuclear spins leading to potential applications in magnetic resonance imaging. Combining these advantages together with the great biocompatibility, NDs have great potential to serve as noninvasive nanosensors for studying the

structure of biomolecules and monitoring biological reactions even inside living organisms. Although this field is just emerging, several successful examples have already been demonstrated and indicated the prospective of ND quantum sensors, which will be discussed in this section.

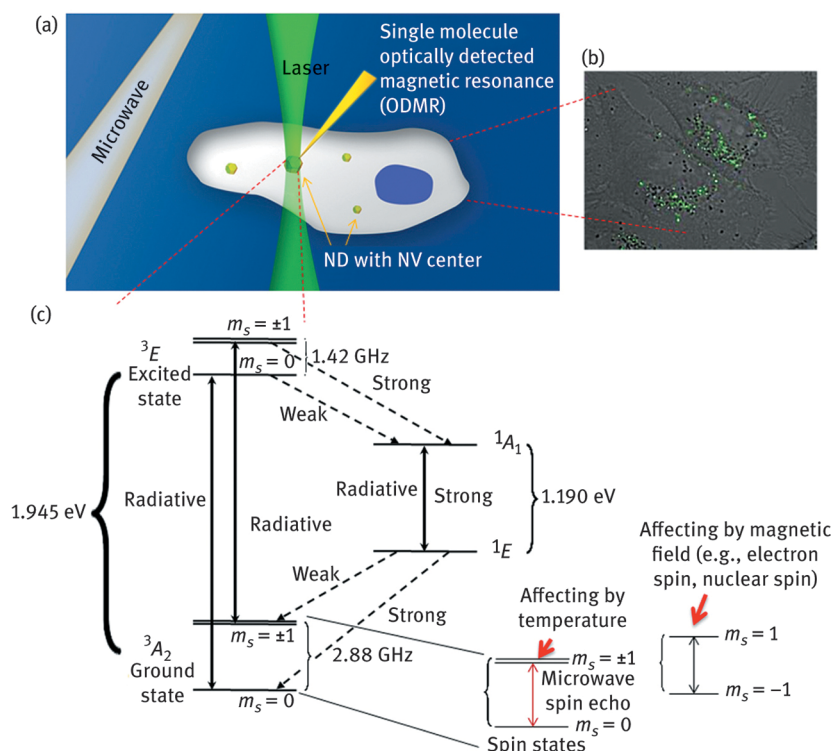


**Figure 8:** Illustration of ND quantum sensing in living cells. (a) The experimental setup for ND quantum sensing inside living cells. (b) Confocal fluorescence microscopy image of NDs with NV centers inside living cells (the bright dots). (c) The energy diagram of NV center. The dangling bonds form an electronic spin-1 system with an optical transition at 1.945 eV. Optical and infrared transition (solid arrows) and weak nonradiative transitions (dashed lines) allow for the observation of spin-dependent fluorescence and optical electron spin polarization. The spin states of ground state for temperature and magnetic sensing are amplified.

### 8.6.1 Fluorescence Imaging with NDs

NDs are emerging as efficient and safe candidates for fluorescent cellular imaging due to their bright fluorescence in the near-infrared region, high photostability with sufficiently long lifetime and excellent biocompatibility. Several studies have investigated FNDs as biomarker for in vitro and in vivo imaging. For instance, ND could serve as fluorescent marker to label biomolecules such as protein. ND-labeled transferrin was imaged by confocal fluorescence microscopy to confirm the receptor-mediated uptake into HeLa cells [43]. Actin and mitochondrial antibody-conjugated NDs were able to label actin and mitochondria in HeLa cells, suggesting the potential of NDs for imaging specific cellular structures [44]. The protein-conjugated NDs were found to exhibit negligible changes with respect to the fluorescence spectra and lifetimes [43]. Moreover, Mohan et al. [9]b] have even imaged the bare FNDs and albumin-conjugated FNDs in *C. elegans* (Figure Figure 9) by differential interference and wide-field epifluorescence microscopic images. The bare NDs were found in the lumen of the worm without intestinal absorption even after 12 h and were fast excreted when the worms were fed *Escherichia coli*. In contrast, albumin-conjugated NDs were taken up by the intestinal cells of the worm and remained there for 24 h, despite *E. coli* feeding. This result indicated that surface functionalization could significantly alter the in vivo fate of NDs. Albumin coating is known to improve the colloidal stability of NDs as discussed in Section 8.3. The enhanced dispersibility of the NDs was believed to be the reason for enhanced cellular uptake. In this study, no photobleaching or photoblinking of NDs was observed even after 48 h of continuous laser excitation, indicating the great potential of FNDs for long-term bioimaging in vivo.

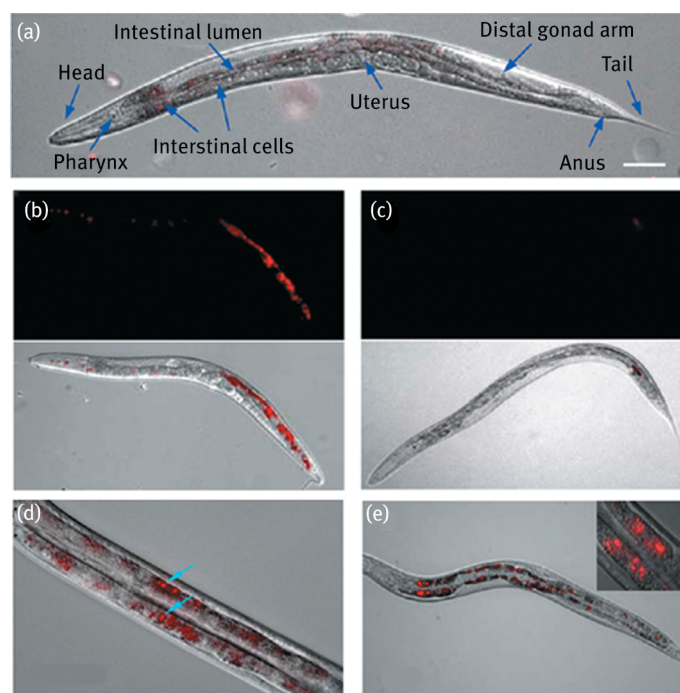


**Figure 9:** Epifluorescence and epifluorescence/DIC-merged images of wild-type *C. elegans*. (A) An untreated young adult. Scale bar: 50  $\mu\text{m}$ . (B) Worms fed with bare FNDs for 12 h. The FNDs stayed inside the gut and were not excreted out when the worms were deprived of food. (C) Worms fed with bare FNDs for 2 h and recovered on to *E. coli* bacterial lawns for 40 min. Almost, if not all, FNDs were excreted out after feeding *E. coli* within 1 h. (D) Worms fed with BSA-coated FNDs for 3 h. FNDs can be seen to be localized within the intestinal cells (solid arrows). (E) Worms fed with BSA-coated FNDs for 3 h and recovered on to *E. coli* bacterial lawns for 1 h. The FNDs staying in the lumen are excreted out, whereas the ones localized in the cells retain. Insets: 100 $\times$  magnified images of the FNDs within the intestinal cells. Anterior is left and dorsal is up in all the figures. Reprinted from Ref. [9]b] with permission.

Furthermore, the high-resolution fluorescence microscopy developed during the past two decades nowadays provides ultimate sensitivity of detection beyond the limits imposed by the diffraction of light. The fluorophores for superresolution imaging techniques are required to be completely photostable without bleaching after long time and strong illumination. Therefore, NDs are particularly attractive for single molecular imaging with these newly developed superresolution fluorescent microscopy. For instance, STED microscopy could image individual NV center in diamond crystals and map the 3D distribution of NV centers with resolution down to 6 nm [45]. Using STED microscopy, single NDs could be tracked in live cells with resolution down to 39 nm [19]. Notably, for such high-resolution fluorescence imaging, coated NDs with good dispersity without aggregation are particularly critical.

### 8.6.2 NDs as Nanoscale Magnetometer

The emission signal from an NV center of NDs is not only attractive for fluorescence imaging, but can also be developed as a magnetometer. As shown in Figure Figure 8, the ground-state spin triplet of NV centers can be coherently manipulated using microwave pulses (spin echo) and efficiently initialized and detected by means of laser illumination. Thus, the energy of spin levels of individual NV centers could serve as fingerprints, allowing identification and tracking of ND particles with identical fluorescence. By this way, individual FNDs could be detected inside living cells with nanoscale precision with regard to their location, orientation, spin levels and spin coherence times [46].

In addition, the triplet ground state of the NV center is sensitive to the changes in the local environment, which could be detected by monitoring decoherence rates. This might provide unique insights into intracellular processes. For instance, ND could be developed as a sensitive nanoscale thermometry [47]. The transition frequency from the singlet ground state to triplet ground state (Figure Figure 8) has a temperature dependence, which could be measured by the change of spin coherent time [47]. With this technique it is possible to noninvasively measure the local temperature in living cells at length scales as short as 200 nm [47].

Moreover, the triplet ground state of the NV center will also be modified by the presence of external spins, which could be recorded as shift of the fluorescence spectral lines or perturbation of the spin echo or changing of the relaxation time of NV centers (Figure Figure 8). For instance, the fast fluctuating external spins generate

noise to the relaxation of NV centers, which could be measured as a signal using decoherence microscopy. The sensitivity of this technique is able to reach the ultimate limit down to the detection of a single paramagnetic ion [48]. Therefore, the NDs could serve as a nanoscale magnetometer that could be delivered into cells and living organisms for electron spin sensing. If a biomolecule is labeled with paramagnetic ions, it could be detected even with single molecular sensitivity [49]. More straightforwardly, this technique is particularly interesting for studying magnetic proteins, which contain paramagnetic ions natively with special functions, such as ferritin. As the major iron reservoir in living organisms, ferritin is a protein cage that could store around 4,500  $\text{Fe}^{3+}$  ions in one particle. Plasma ferritin concentration and the amount of iron inside ferritin is an important marker for many diseases such as anemia, hypothyroidism and celiac disease. The detection of ferritin with NDs is based on magnetic noise induced by the paramagnetic iron at the interior. When ferritins are adsorbed on the surface of NDs, a significant reduction of both coherence ( $T_2$ ) and relaxation time ( $T_1$ ) could be obtained and the detection sensitivity is found to be able to reach the single molecule detection threshold [28, 50] (Figure Figure 10). Since NDs are also ideal carriers to deliver biomolecules of interest into cells and living organisms as discussed earlier, one could envision a nanoscopic electron spin sensor for detection of electron spin containing biomolecules in vitro and in vivo. Furthermore, the remarkable sensitivity paired with the noninvasive character of NDs may also provide access to quantum mechanical studies in living organisms, which may have potential to resolve important electron transfer process and radical pair dynamics in cellular environments [51].

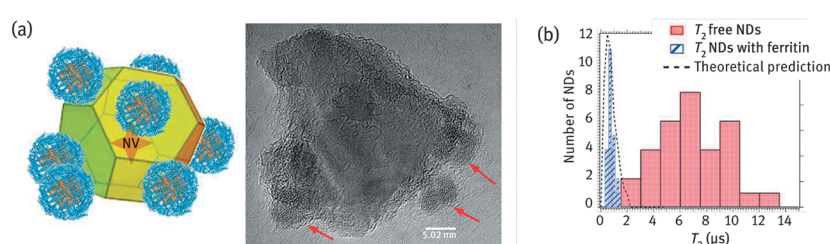


**Figure 10:** Detection of iron ions inside ferritin with fluorescent NDs. (a) Illustration of the ferritin adsorbed on fluorescent NDs and the TEM visualization. (b) The changing of  $T_2$  time in response to iron ions in ferritin. Reprinted from Ref. [28] with permission.

Similar like sensing of electron spin, the magnetic field from a nuclear spin could also induce changes on the triplet ground state of NV centers thus being detected optically (Figure Figure 8). However, a single nuclear magnetic moment is approximately 1,000 times weaker than an electron spin. To detect such weak signal, the nuclear spin needs to be brought into close proximity to the NV center (a few nanometers) to produce sufficient field in the order of microtesla. In addition, using high order of spin echoes, for example, generated by microwave, the coherence time of NV defects in the presence of nuclear spins can be improved by orders of magnitude [52]. By this way, the NV centers could have great potential for developing nanoscale nuclear magnetic resonance (NMR) spectroscopy ultimately with even single molecular sensitivity [53]. Recently, the detection of proton NMR in only  $5 \text{ nm}^3$  volume of liquid sample was achieved by directly placing the sample on single NV centers implanted 2.5–10 nm below the diamond surface [54]. By constructing a microfluidic device on diamond, picoliter-scale sample could be easily applied to allow detection of the nuclear spin in solution with below 500 nm spatial resolution [55]. Single nuclear spin inside solid sample with long coherence time, such as Si29 in quartz and nuclear spins associated with hydrogen bound to diamond interface, could also be detected within a few seconds measurement time if the solid sample is directly placed on diamond surface [56]. Although the successful experiments are still based on NV centers implanted inside bulk diamonds, the same strategy should also be able to realize nuclear spin detection with NDs. However, it is much more challenging to manipulate a single NV center in ND and attach the molecule of interest within a few nanometer distance from the NV center. In addition, currently only location and intensity of the nuclear spin could be determined by the NV-based NMR technique. For more useful applications, such as the elucidation of biomolecule structures, the spectral resolution should be further improved in order to detect dipolar couplings and chemical shifts. Several strategies might be helpful in this respect, such as the development of new measurement protocols similar to 2D NMR [57], or new protocols to remove magnetic noise that are developed in the context of quantum computations (e.g., quantum error correction) [58].

### 8.6.3 Magnetic Resonance Imaging with Hyperpolarized NDs

Magnetic resonance imaging (MRI) is one of the most important diagnostic techniques allowing noninvasive imaging of tissue and organs inside the body. However, the sensitivity of MRI is only sufficient to detect large defects in tissue, which limits its applications for early diagnostic of important disease. This low sensitivity is

partially related to low polarization of nuclear spins at low temperature. The electron spin native to the NV center can be initialized to a highly polarized quantum state by laser irradiation on microsecond timescale, which is known as hyperpolarization technique. This polarization can then be transferred to surrounding nuclear spins with the support of microwave radiation, thus to achieve hyperpolarized nuclear spins at room temperature [59]. This technique has emerged as a new approach for accessing highly sensitive MRI that might be sufficient for even single molecule detection [60]. The relaxation time of hyperpolarized NV centers in bulk diamond could reach hours. However, the polarization of diamond nanoparticles represents a more challenging task due to the more disordered orientation of NV centers. Advanced dynamic nuclear spin polarization protocols developed recently are able to address this problem [61]. With this method, it has been shown that the relaxation time of hyperpolarized NDs could also reach more than a minute, which is superior to any known MRI contrast agent. Furthermore, the polarization of NV centers can also be transferred to external nuclear spins if they are located close to the diamond surface [62]. Thus, by constructing flow channels with hyperpolarized diamond, the molecules in a tiny volume could be highly polarized, which might provide another mechanism for developing ultrasensitive NMR [63].

## 8.7 Conclusions

In summary, ND as one of the most biocompatible nanoparticles provides great potential for a broad range of biological applications, including bioimaging, drug delivery and quantum sensing. Compared to other carbon nanomaterials, such as carbon nanotubes, NDs were found to be biocompatible in vitro and in vivo. Although the strong aggregation inside biological systems represents one of the main limitations of NDs, many coating strategies including polymer and silica coatings have been already developed to achieve highly stable NDs with even better biocompatibility. Functional molecules, such as protein, DNA and drug molecules, could be conjugated to NDs via both physical adsorption and covalent conjugation chemistries. Based on these preparation methods, NDs are ready to be flexibly tailored as multifunctional drug delivery carrier. A large variety of drug molecules have been delivered with NDs and shown increased therapeutic efficiency and reduced systematic toxicity in vitro and in vivo. Particularly, with the excellent fluorescence and electromagnetic properties, NDs offer unique potential for bioimaging and sensing with different optical and quantum approaches. The highly stable near-infrared fluorescence of NV centers inside NDs is essential for advanced high-resolution fluorescence imaging in cells and tissue. The special electron spin states of NV centers in NDs enable unlimited potential for developing nanoscale quantum sensors for detection of the tiniest changes of magnetic fields, external electron and magnetic spins as well as temperature under biological environment. These techniques might eventually allow detection and analysis of structure, dynamics and function of single biomolecule under native conditions with high sensitivity and nanometer spatial resolution. Hyperpolarization of NV centers also offered great opportunity to develop high-resolution MRI that might be able to reach molecular detection sensitivity. The combination of these bioimaging techniques with drug delivery capability of NDs would be promising for next-generation theranostics to allow sensitive multimode diagnostic together with targeted drug therapy within one nanoparticle.

It should be stressed that several challenges still need to be addressed before these highly promising techniques could be really brought into clinical benefit. Particularly for the auspicious electromagnetic quantum sensing, a variety of challenges still need to be overcome. For instance, ND sensors with single molecular detection sensitivity will be easily perturbed by even weak noise such as nuclear and electron spins, charges and radicals in random motion, which are intrinsically present in biological systems. Furthermore, the ND sensor is not stationary. The fast movement and rotation leads to randomization of the signals. Several theoretical solutions for these challenges have been already developed, but need to be further verified experimentally in biological environment, even though current studies have already established the fundamental basis of these quantum-sensing techniques, which are highly promising to be brought into the application level in the near future.

## Acknowledgments

Tanja Weil und Ihre Gruppe danken Frau Kalkhof-Rose für Ihr großes Interesse und Ihre freundliche Förderung unserer Forschung an Nanodiamanten für die biomedizinische Forschung. In addition, the authors thank Sean Harvey for proof-reading.

This article is also available in: Muellen, Feng, Chemistry of Carbon Nanostructures. De Gruyter (2016), isbn 978-3-11-028450-8.

## References

- [1] Shenderova OA, Gruen DM. Ultrananocrystalline diamond: synthesis, properties and applications. William Andrew, New York, 2012.
- [2] (a) Boudou JP, Curmi PA, Jelezko F, Wrachtrup J, Aubert P, Sennour M, et al. High yield fabrication of fluorescent nanodiamonds. *Nanotechnology* 2009;20(23): 235602; (b) Boudou J-P, Tisler J, Reuter R, Thorel A, Curmi PA, Jelezko F, et al. Fluorescent nanodiamonds derived from HPHT with a size of less than 10 nm. *Diamond Relat Mater* 2013;37:80–6. [2] Boudou J-P, Tisler J, Reuter R, Thorel A, Curmi PA, Jelezko F. Fluorescent nanodiamonds derived from HPHT with a size of less than 10 nm. *Diamond Relat Mater* 2013;37:80–86.
- [3] Zaitsev AM. Optical properties of diamond: a data handbook. Springer, New York, 2001.
- [4] Doherty MW, Manson NB, Delaney P, Jelezko F, Wrachtrup J, Hollenberg LC. The nitrogen-vacancy colour centre in diamond. *Phys Rep* 2013;528(1):1–45.
- [5] Fu C-C, Lee H-Y, Chen K, Lim T-S, Wu H-Y, Lin P-K, et al. Characterization and application of single fluorescent nanodiamonds as cellular biomarkers. *Eur Spine J* 2010;19(5):754–9.
- [6] Balasubramanian G, Neumann P, Twitchen D, Markham M, Kolesov R, Mizuochi N, et al. Ultralong spin coherence time in isotopically engineered diamond. *Nat Mater* 2009;8(5):383–7.
- [7] Schrand AM, Huang H, Carlson C, Schlager JJ, Osawa E, Hussain SM, et al. Are diamond nanoparticles cytotoxic? *J Phys Chem B* 2007;111(1):2–7.
- [8] (a) Yuzhou W, Fedor J, Martin BP, Tanja W. Diamond quantum sensing in biology. *Angew Chem Int Ed* 2016; 55(23):6586–98; (b) Vajjayanthimala V, Chang HC. Functionalized fluorescent nanodiamonds for biomedical applications. *Nanomedicine* 2008;4(1):47–55; (c) Mochalin VN, Shenderova O, Ho D, Gogotsi Y. The properties and applications of nanodiamonds. *Nat Nano* 2012;7(1):11–23. [8] Vajjayanthimala V, Chang HC. Functionalized fluorescent nanodiamonds for biomedical applications. *Nanomedicine* 2008;4(1):47–55. [8] Mochalin VN, Shenderova O, Ho D, Gogotsi Y. The properties and applications of nanodiamonds. *Nat Nano* 2012;7(1):11–23.
- [9] (a) Vajjayanthimala V, Cheng P-Y, Yeh S-H, Liu K-K, Hsiao C-H, Chao J-I, et al. The long-term stability and biocompatibility of fluorescent nanodiamond as an in vivo contrast agent. *Biomaterials* 2012;33(31):7794–802; (b) Mohan N, Chen C-S Hsieh H-H, Wu YC, Chang H-C. In vivo imaging and toxicity assessments of fluorescent nanodiamonds in *Caenorhabditis elegans*. *Nano Lett* 2010;10(9):3692–9; (c) Liu K-K, Cheng C-L, Chang C-C, Chao J. Biocompatible and detectable carboxylated nanodiamond on human cell. *Nanotechnology* 2007;18(32):325102; (d) Schrand AM, Dai L, Schlager JJ, Hussain SM, Osawa E. Differential biocompatibility of carbon nanotubes and nanodiamonds. *Diamond Relat Mater* 2007;16(12):2118–23. [9] Mohan N, Chen C-S, Hsieh H-H, Wu YC, Chang H-C. In vivo imaging and toxicity assessments of fluorescent nanodiamonds in *Caenorhabditis elegans*. *Nano Lett* 2010;10(9):36923699. [9] Liu K-K, Cheng C-L, Chang C-C, Chao J. Biocompatible and detectable carboxylated nanodiamond on human cell. *Nanotechnology* 2007;18(32):325102. [9] Schrand AM, Dai L, Schlager JJ, Hussain SM, Osawa E. Differential biocompatibility of carbon nanotubes and nanodiamonds. *Diamond Relat Mater* 2007;16(12):2118–2123.
- [10] (a) Xing Y, Xiong W, Zhu L, Osawa E, Hussain S, Dai L. DNA damage in embryonic stem cells caused by nanodiamonds. *ACS Nano* 2011;5(3):2376–84; (b) Yuan Y, Chen Y, Liu J-H, Wang H, Liu Y. Biodistribution and fate of nanodiamonds in vivo. *Diamond Relat Mater* 2009;18(1):95–100. [10] Yuan Y, Chen Y, Liu J-H, Wang H, Liu Y. Biodistribution and fate of nanodiamonds in vivo. *Diamond Relat Mater* 2009;18(1):95–100.
- [11] (a) Moore L, Grobarova V, Shen H, Man HB, Micova J, Ledvina M, et al. Comprehensive interrogation of the cellular response to fluorescent, detonation and functionalized nanodiamonds. *Nanoscale* 2014;6(20):11712–21; (b) Batsanov SS, Gavrilkin SM, Batsanov AS, Poyarkov KB, Kulakova II, Johnson DW, et al. Giant dielectric permittivity of detonation-produced nanodiamond is caused by water. *J Mater Chem* 2012;22(22):11166–72. [11] Batsanov SS, Gavrilkin SM, Batsanov AS, Poyarkov KB, Kulakova II, Johnson DW, et al. Giant dielectric permittivity of detonation-produced nanodiamond is caused by water. *J Mater Chem* 2012;22(22):11166–72.
- [12] Liu K-K, Wang C-C, Cheng C-L, Chao J-I. Endocytic carboxylated nanodiamond for the labeling and tracking of cell division and differentiation in cancer and stem cells. *Biomaterials* 2009;30(26):4249–59.
- [13] Krueger A, Lang D. Functionality is key: recent progress in the surface modification of nanodiamond. *Adv Funct Mater* 2012;22(5):890–906.
- [14] Price ME, Cornelius RM, Brash JL. Protein adsorption to polyethylene glycol modified liposomes from fibrinogen solution and from plasma. *Biochim Biophys Acta Biomembr* 2001;1512(2):191–205.
- [15] (a) Zhang X, Fu C, Feng L, Ji Y, Tao L, Huang Q, Li S, Wei Y. PEGylation and polyPEGylation of nanodiamond. *Polymer* 2012;53(15):3178–84; (b) Wang D, Tong Y, Li Y, Tian Z, Cao R, Yang B. PEGylated nanodiamond for chemotherapeutic drug delivery. *Diamond Relat Mater* 2013;36:26–34; (c) Zhao L, Xu Y-H, Qin H, Abe S, Akasaka T, Chano T, et al. Platinum on nanodiamond: a promising prodrug conjugated with stealth polyglycerol, targeting peptide and acid-responsive antitumor drug. *Adv Funct Mater* 2014;24(34):5348–57; (d) Rehorl I, Mackova H, Filippov SK, Kucka J, Proks V, Sleggerova J, Turner S, Van Tendeloo G, Ledvina M, Hruby M, Cigler P. Fluorescent Nanodiamonds with Bioorthogonally Reactive Protein-Resistant Polymeric Coatings. *ChemPlusChem* 2014;79(1):21–4. [15] Wang D, Tong Y, Li Y, Tian Z, Cao R, Yang B. PEGylated nanodiamond for chemotherapeutic drug delivery. *Diamond Relat Mater* 2013;36:26–34. [15] Zhao L, Xu Y-H, Qin H, Abe S, Akasaka T, Chano T, et al. Platinum on nanodiamond: a promising prodrug conjugated with stealth polyglycerol, targeting peptide and acid-responsive antitumor drug. *Adv Funct Mater* 2014;24(34):5348–57. [15] Rehorl I, Mackova H, Filippov SK, Kucka J, Proks V, Sleggerova J, Turner S, Van Tendeloo G, Ledvina M, Hruby M, Cigler P. Fluorescent Nanodiamonds with Bioorthogonally Reactive Protein-Resistant Polymeric Coatings. *ChemPlusChem* 2014;79(1):21–4.
- [16] Zhao L, Takimoto T, Ito M, Kitagawa N, Kimura T, Komatsu N. Chromatographic separation of highly soluble diamond nanoparticles prepared by polyglycerol grafting. *Angew Chem Int Ed* 2011;50(6):1388–92.
- [17] Barras A, Lyskawa J, Szunerits S, Woisel P, Boukherroub R. Direct functionalization of nanodiamond particles using dopamine derivatives. *Langmuir* 2011;27(20):12451–7.
- [18] Kong XL, Huang LCL, Hsu CM, Chen WH, Han CC, Chang HC. High-affinity capture of proteins by diamond nanoparticles for mass spectrometric analysis. *Anal Chem* 2005;77(1) 259–65.

- [19] Tzeng Y-K, Faklaris O, Chang B-M, Kuo Y, Hsu J-H, Chang H-C Superresolution imaging of albumin-conjugated fluorescent nanodiamonds in cells by stimulated emission depletion. *Angew Chem Int Ed* 2011;50(10):2262–5.
- [20] Zhang X-Q, Chen M, Lam R, Xu X, Osawa E, Ho D. Polymer-functionalized nanodiamond platforms as vehicles for gene delivery. *ACS Nano* 2009;3(9):2609–16.
- [21] (a) Slegerova J, Hajek M, Rehor I, Sedlak F, Stursa J, Hruby M, Cigler P. Designing the nanobiointerface of fluorescent nanodiamonds: highly selective targeting of glioma cancer cells. *Nanoscale* 2015;7(2):415–20; (b) Wu Y, Ermakova A, Liu W, Pramanik G, Vu TM, Kurz A, et al. Programmable biopolymers for advancing biomedical applications of fluorescent nanodiamonds. *Adv Funct Mater* 2015;25(42):6576–85. [21] WuY, ErmakovaA, LiuW, PramanikG, VuTM, KurzA, Programmable biopolymers for advancing biomedical applications of fluorescent nanodiamonds. *Adv Funct Mater* 2015;25(42):6576–85.
- [22] (a) Wu Y, Chakraborty S, Gropeanu RA, Wilhelm J, Xu Y, Er KS, et al. pH-responsive quantum dots via an albumin polymer surface coating. *J Am Chem Soc* 2010;132(14):5012–14; (b) Wu Y, Pramanik G, Eisele K, Weil T. Convenient approach to polypeptide copolymers derived from native proteins. *Biomacromolecules* 2012;13(6):1890–8. [22] WuY, PramanikG, EiseleK, WeilT. Convenient approach to polypeptide copolymers derived from native proteins. *Biomacromolecules* 2012;13(6):1890–8.
- [23] Bumb A, Sarkar SK, Billington N, Brechbiel MW, Neuman KC. Silica encapsulation of fluorescent nanodiamonds for colloidal stability and facile surface functionalization. *J Am Chem Soc* 2013;135(21):7815–18.
- [24] Rehor I, Slegerova J, Kucka J, Proks V, Petrakova V, Adam M-P, et al. Fluorescent nanodiamonds embedded in biocompatible translucent shells. *Small* 2014;10(6):1106–15.
- [25] Rehor I, Mackova H, Filippov SK, Kucka J, Proks V, Slegerova J, et al. Fluorescent nanodiamonds with bioorthogonally reactive protein-resistant polymeric coatings. *ChemPlusChem* 2014;79(1):21–4.
- [26] Shimkunas RA, Robinson E, Lam R, Lu S, Xu X, Zhang X-Q, et al. Nanodiamond–insulin complexes as pH-dependent protein delivery vehicles. *Biomaterials* 2009;30(29):5720–8.
- [27] Chang B-M, Lin H-H, Su L-J, Lin W-D, Lin R-J, Tzeng Y-K, et al. Highly fluorescent nanodiamonds protein-functionalized for cell labeling and targeting. *Adv Funct Mater* 2013;23(46):5737–45.
- [28] Ermakova A, Pramanik G, Cai JM, Algara-Siller G, Kaiser U, Weil T, et al. Detection of a few metallo-protein molecules using color centers in nanodiamonds. *Nano Lett* 2013;13(7):3305–9.
- [29] Krueger A. The structure and reactivity of nanoscale diamond. *J Mater Chem* 2008;18(13):1485–92.
- [30] Zhang X-Q, Lam R, Xu X, Chow EK, Kim H-J, Ho D. Multimodal nanodiamond drug delivery carriers for selective targeting imaging and enhanced chemotherapeutic efficacy. *Adv Mater* 2011;23(41):4770–5.
- [31] Zhang T, Neumann A, Lindlau J, Wu Y, Pramanik G, Naydenov B, et al. DNA-based self-assembly of fluorescent nanodiamonds. *J Am Chem Soc* 2015;137(31):9776–9.
- [32] Albrecht A, Koplovitz G, Retzker A, Jelezko F, Yochelis S, Porath D, et al. Self-assembling hybrid diamond–biological quantum devices. *New J Phys* 2014;16(9):093002.
- [33] Rothmund PW. Folding DNA to create nanoscale shapes and patterns. *Nature* 2006;440(7082):297–302.
- [34] Huang H, Pierstorff E, Osawa E, Ho D. Active nanodiamond hydrogels for chemotherapeutic delivery. *Nano Lett* 2007;7(11):3305–14.
- [35] (a) Chow EK, Zhang X-Q, Chen M, Lam R, Robinson E, Huang H, et al. Nanodiamond therapeutic delivery agents mediate enhanced chemoresistant tumor treatment. *Sci Transl Med* 2011;3(73):73ra21; (b) Xiao J, Duan X, Yin Q, Zhang Z, Yu H, Li Y. Nanodiamonds-mediated doxorubicin nuclear delivery to inhibit lung metastasis of breast cancer. *Biomaterials* 2013;34(37):9648–56. [35] XiaoJ, DuanX, YinQ, ZhangZ, YuH, LiY. Nanodiamonds-mediated doxorubicin nuclear delivery to inhibit lung metastasis of breast cancer. *Biomaterials* 2013;34(37):9648–56.
- [36] Chen M, Pierstorff ED, Lam R, Li SY, Huang H, Osawa E, et al. Nanodiamond-mediated delivery of water-insoluble therapeutics. *ACS Nano* 2009;3(7):2016–22.
- [37] Toh TB, Lee DK, Hou W, Abdullah LN, Nguyen J, Ho D, Chow EK. Nanodiamond-mitoxantrone complexes enhance drug retention in chemoresistant breast cancer cells. *Mol Pharm* 2014;11(8):2683–91.
- [38] Li X, Shao J, Qin Y, Shao C, Zheng T, Ye L. TAT-conjugated nanodiamond for the enhanced delivery of doxorubicin. *J Mater Chem* 2011;21(22):7966–73.
- [39] Liu KK, Zheng WW, Wang CC, Chiu YC, Cheng CL, Lo YS, et al. Covalent linkage of nanodiamond-paclitaxel for drug delivery and cancer therapy. *Nanotechnology* 2010;21(31):315106.
- [40] Azad N, Rojanasakul Y. Nanobiotechnology in drug delivery. *Am J Drug Delivery* 2012;4(2):79–88.
- [41] Wrachtrup J, von Borczyskowski C, Bernard J, Orritt M, Brown R. Optical detection of magnetic resonance in a single molecule. *Nature* 1993;363(6426):244–5.
- [42] Gruber A, Dräbenstedt A, Tietz C, Fleury L, Wrachtrup J, Borczyskowski Cv. Scanning confocal optical microscopy and magnetic resonance on single defect centers. *Science* 1997;276(5321):2012–14.
- [43] Weng M-F, Chiang S-Y, Wang N-S, Niu H. Fluorescent nanodiamonds for specifically targeted bioimaging: application to the interaction of transferrin with transferrin receptor. *Diamond Relat Mater* 2009;18(2–3):587–91.
- [44] Mkandawire M, Pohl A, Gubarevich T, Lapina V, Appelhans D, Rödel G, et al. Selective targeting of green fluorescent nanodiamond conjugates to mitochondria in HeLa cells. *J Biophoton* 2009;2(10):596–606.
- [45] (a) Rittweger E, Han KY, Irvine SE, Eggeling C, Hell SW. STED microscopy reveals crystal colour centres with nanometric resolution. *Nat Photon* 2009;3(3):144–7; (b) Han KY, Willig KI, Rittweger E, Jelezko F, Eggeling C, Hell SW. Three-Dimensional Stimulated Emission Depletion Microscopy of Nitrogen-Vacancy Centers in Diamond Using Continuous-Wave Light. *Nano Letters* 2009 9 (9) 3323–9; (c) Arroyo-Camejo S, Adam M. P, Besbes M, Hugonin J. P, Jacques V, Greffet J. J, Roch J. F Hell S. W Treussart F. Stimulated Emission Depletion Microscopy resolves individual nitrogen vacancy centers in diamond nanocrystals. *ACS Nano* 2013;7(12):10912–19. [45] HanKY, WilligKI, RittwegerE, JelezkoF, EggelingC, HellSW. Three-Dimensional Stimulated Emission Depletion Microscopy of Nitrogen-Vacancy Centers in Diamond Using Continuous-Wave Light. *Nano Letters* 2009;9(9):3323–9. [45] Arroyo-CamejoS, AdamM.P, BesbesM, HugoninJ.P, JacquesV, GreffetJ.J, RochJ.F, HellS.W, TreussartF. Stimulated Emission Depletion Microscopy resolves individual nitrogen vacancy centers in diamond nanocrystals. *ACS Nano* 2013;7(12):10912–19.

- [46] Maze JR, Stanwix PL, Hodges JS, Hong S, Taylor JM, Cappellaro P, et al. Nanoscale magnetic sensing with an individual electronic spin in diamond. *Nature* 2008;455(7213):644–U41.
- [47] Kucsko G, Maurer PC, Yao NY, Kubo M, Noh HJ, Lo PK, et al. Nanometre-scale thermometry in a living cell. *Nature* 2013;500(7460):54–8.
- [48] Sushkov AO, Chisholm N, Lovchinsky I, Kubo M, Lo PK, Bennett SD, et al. All-optical sensing of a single-molecule electron spin. *Nano Lett* 2014;14(11):6443–8.
- [49] Shi FZ, Zhang Q, Wang PF, Sun HB, Wang JR, Rong X, et al. Single-protein spin resonance spectroscopy under ambient conditions. *Science* 2015;347(6226):1135–8.
- [50] Schafer-Nolte E, Schlipf L, Ternes M, Reinhard F, Kern K, Wrachtrup J. Tracking temperature-dependent relaxation times of ferritin nanomagnets with a wideband quantum spectrometer. *Phys Rev Lett* 2014;113(21).
- [51] Huelga SF, Plenio MB. Vibrations, quanta and biology. *Contemp Phys* 2013;54:181–207.
- [52] Romach Y, Muller C, Unden T, Rogers LJ, Isoda T, Itoh KM, et al. Spectroscopy of surface-induced noise using shallow spins in diamond. *Phys Rev Lett* 2015;114(1):017601.
- [53] Lovchinsky I, Sushkov AO, Urbach E, de Leon NP, Choi S, De Greve K, et al. Nuclear magnetic resonance detection and spectroscopy of single proteins using quantum logic. *Science* 2016;351(6275):836–41.
- [54] (a) Staudacher T, Shi F, Pezzagna S, Meijer J, Du J, Meriles CA, et al. Nuclear magnetic resonance spectroscopy on a (5-nanometer)<sup>3</sup> sample volume. *Science* 2013;339(6119):561–3; (b) Mamin HJ, Kim M, Sherwood MH, Rettner CT, Ohno K, Awschalom DD, Rugar D. Nanoscale nuclear magnetic resonance with a nitrogen-vacancy spin sensor. *Science* 2013;339(6119):557–60. [54] Mamin HJ, Kim M, Sherwood MH, Rettner CT, Ohno K, Awschalom DD, Rugar D. Nanoscale nuclear magnetic resonance with a nitrogen-vacancy spin sensor. *Science*. 2013;339(6119):557–60.
- [55] Steinert S, Ziem F, Hall LT, Zappe A, Schweikert M, Götz N, et al. Magnetic spin imaging under ambient conditions with sub-cellular resolution. *Nat Commun* 2013;4:1607.
- [56] Muller C, Kong X, Cai JM, Melentijevic K, Stacey A, Markham M, et al. Nuclear magnetic resonance spectroscopy with single spin sensitivity. *Nat Commun* 2014;5:4703.
- [57] Ajoy A, Bissbort U, Lukin MD, Walsworth RL, Cappellaro P Atomic-scale nuclear spin imaging using quantum-assisted sensors in diamond *Phys Rev X* 2015;5:011001; (b) Kost M, Cai J, Plenio MB. Resolving single molecule structures with Nitrogen-vacancy centers in diamond. *Sci Rep* 2015;5:11007. [57] Kost M, Cai J, Plenio MB. Resolving single molecule structures with Nitrogen-vacancy centers in diamond. *Sci Rep*. 2015;5:11007.
- [58] (a) Kessler EM, Lovchinsky I, Sushkov AO, Lukin MD. Quantum error correction for metrology. *Phys Rev Lett* 2014;112(15):150802; (b) Arrad G, Vinkler Y, Aharonov D, Retzker A. Increasing sensing resolution with error correction. *Physical Rev Lett* 2014;112(15):150801. [58] Arrad G, Vinkler Y, Aharonov D, Retzker A. Increasing sensing resolution with error correction. *Physical Rev Lett*. 2014;112(15):150801.
- [59] (a) Scheuer J, Schwartz I, Chen Q, Schulzesünninghausen D, Carl P, Höfer P, et al. Optically induced dynamic nuclear spin polarisation in diamond. *New J Phys* 2016;18(1):013040; (b) London P, Scheuer J, Cai JM, Schwarz I, Retzker A, Plenio MB, et al. Detecting and polarizing nuclear spins with double resonance on a single electron spin. *Phys Rev Lett* 2013;111(6):067601; (c) King JP, Jeong K, Vassiliou CC, Shin CS, Page RH, Avalos CE, et al. Room-temperature in situ nuclear spin hyperpolarization from optically pumped nitrogen vacancy centres in diamond. *Nat Commun* 2015;6:8965; (d) Fischer R, Bretschneider CO, London P, Budker D, Gershoni D, Frydman L. Bulk nuclear polarization enhanced at room temperature by optical pumping. *Phys Rev Lett* 2013;111(5). [59] London P, Scheuer J, Cai JM, Schwarz I, Retzker A, Plenio MB. Detecting and polarizing nuclear spins with double resonance on a single electron spin. *Phys Rev Lett*. 2013;111(6):067601. [59] King JP, Jeong K, Vassiliou CC, Shin CS, Page RH, Avalos CE. Room-temperature in situ nuclear spin hyperpolarization from optically pumped nitrogen vacancy centres in diamond. *Nat Commun*. 2015;6:8965. [59] Fischer R, Bretschneider CO, London P, Budker D, Gershoni D, Frydman L. Bulk nuclear polarization enhanced at room temperature by optical pumping. *Phys Rev Lett*. 2013;111(5).
- [60] (a) Dutta P, Martinez GV, Gillies RJ. Nanodiamond as a new hyperpolarizing agent and its C-13 MRS. *J Phys Chem Lett* 2014;5(3):597–600; (b) Chen Q, Schwarz I, Jelezko F, Retzker A, Plenio MB. Optical hyperpolarization of <sup>13</sup>C nuclear spins in nanodiamond ensembles. *Phys Rev B* 2015;92(18):184420; (c) Jochen S, Ilai S, Qiong C, David S-S, Patrick C, Peter H, et al. Optically induced dynamic nuclear spin polarisation in diamond. *New J Phys* 2016;18(1):013040. [60] Chen Q, Schwarz I, Jelezko F, Retzker A, Plenio MB. Optical hyperpolarization of <sup>13</sup>C nuclear spins in nanodiamond ensembles. *Phys Rev B*. 2015;92(18):184420. [60] Jochen S, Ilai S, Qiong C, David S-S, Patrick C, Peter H, et al. Optically induced dynamic nuclear spin polarisation in diamond. *New J Phys*. 2016;18(1):013040.
- [61] Rej E, Gaebel T, Boele T, Waddington DE, Reilly DJ. Hyperpolarized nanodiamond with long spin-relaxation times. *Nat Commun* 2015;6:8459.
- [62] Abrams D, Trusheim ME, Englund DR, Shattuck MD, Meriles CA. Dynamic nuclear spin polarization of liquids and gases in contact with nanostructured diamond. *Nano Lett* 2014;14(5):2471–8.
- [63] Chen Q, Schwarz I, Jelezko F, Retzker A, Plenio MB. Resonance-inclined optical nuclear spin polarization of liquids in diamond structures. *Phys Rev B* 2016;93(6):060408.